LINC01089 governs the miR-1287-5p/HSPA4 axis to negatively regulate osteogenic differentiation of mesenchymal stem cells

From Xiangyang Hospital of Integrated Traditional Chinese and Western Medicine, Xiangyang, China

Cite this article:
Bone Joint Res 2024;13(12):
779–789.

DOI: 10.1302/2046-3758.
1312.BJR-2023-0272.R2

Correspondence should be sent to Aofei Yang
whyangaofei@163.com

H. Zou,[1] F. Hu,[1] X. Wu,[1] B. Xu,[1] G. Shang,[1] D. An,[1] D. Qin,[1] X. Zhang,[1] A. Yang[2,3]

[1]Department of Orthopedics, Xiangyang Hospital of Integrated Traditional Chinese and Western Medicine, Xiangyang, China
[2]Department of Orthopedics, Hubei Provincial Hospital of Traditional Chinese Medicine, Wuhan, China
[3]Department of Orthopedics, Affiliated Hospital of Hubei University of Chinese Medicine, Wuhan, China

Aims

The involvement of long non-coding RNA (lncRNA) in bone marrow mesenchymal stem cell (MSC) osteogenic differentiation during osteoporosis (OP) development has attracted much attention. In this study, we aimed to disclose how LINC01089 functions in human mesenchymal stem cell (hMSC) osteogenic differentiation, and to study the mechanism by which LINC01089 regulates MSC osteogenesis.

Methods

Quantitative reverse transcription polymerase chain reaction (RT-qPCR) and western blotting were performed to analyze LINC01089, miR-1287-5p, and heat shock protein family A (HSP70) member 4 (HSPA4) expression. The osteogenic differentiation of MSCs was assessed through alkaline phosphatase (ALP) activity, alizarin red S (ARS) staining, and by measuring the levels of osteogenic gene marker expressions using commercial kits and RT-qPCR analysis. Cell proliferative capacity was evaluated via the Cell Counting Kit-8 (CCK-8) assay. The binding of miR-1287-5p with LINC01089 and HSPA4 was verified by performing dual-luciferase reporter and RNA immunoprecipitation (RIP) experiments.

Results

LINC01089 expression was reinforced in serum samples of OP patients, but it gradually diminished while hMSCs underwent osteogenic differentiation. LINC01089 knockdown facilitated hMSC osteogenic differentiation. This was substantiated by: the increase in ALP activity; ALP, runt-related transcription factor 2 (RUNX2), osteocalcin (OCN), and osteopontin (OPN) messenger RNA (mRNA) levels; and level of ARS staining. Meanwhile, LINC01089 upregulation resulted in the opposite effects. LINC01089 targeted miR-1287-5p, and the LINC01089 knockdown-induced hMSC osteogenic differentiation was repressed by miR-1287-5p depletion. HSPA4 is a downstream function molecule of the LINC01089/miR-1287-5p pathway; miR-1287-5p negatively modulated HSPA4 levels and attenuated its functional effects.

Conclusion

LINC01089 negatively regulated hMSC osteogenic differentiation, at least in part, via governing miR-1287-5p/HSPA4 signalling. These findings provide new insights into hMSC osteogenesis and bone metabolism.

Article focus

- We aimed to disclose how LINC01089 functions in human mesenchymal stem cell (hMSC) osteogenic differentiation, and explore the mechanism by which LINC01089 regulates MSC osteogenesis.

Key messages

- LINC01089 negatively regulates hMSC osteogenic differentiation.
- miR-1287-5p is targeted by LINC01089 and negatively regulated by LINC0089, reversing the effect of LINC01089 deficiency.
- Heat shock protein family A (HSP70) member 4 (HSPA4) is a downstream gene of the LINC01089/miR-1287-5p pathway, and inhibition of miR-1287-56p eliminates the knockout effect of HSPA4.

Strengths and limitations

- Our research results reveal for the first time the function of LINC01089 in hMSC osteogenic differentiation, providing a basis for the involvement of LINC01089 in osteoporosis (OP) development.
- The functional role of HSPA4 in MSC osteogenic differentiation requires further exploration.

Introduction

Osteoporosis (OP) has been recognized as a major public health problem, as its prevalence increases with the ageing of the population.[1] When the balance between bone formation and bone resorption is disturbed, progressive bone loss resulting from an increase in the ratio of bone resorption to bone formation can lead to a degenerative bone metabolic disease known as OP.[2] It is characterized by decreased bone resorption, impaired bone mineral density, bone microstructure degradation, and increased bone fragility and fracture risk.[3,4] Currently, a therapeutic strategy considered for OP is the promotion of the osteogenic differentiation among bone marrow mesenchymal stem cells (MSCs).[5] In view of this, it is important to uncover the molecular mechanisms and factors affecting MSC osteogenic differentiation.

Non-coding RNAs (ncRNAs) execute a wide range of functional effects and have regulatory potential in a variety of human diseases. Long non-coding RNA (lncRNA), a class of ncRNA molecules, is implicated in several biological processes such as epigenetics, transcription, translation, and protein modification.[6] Liu et al[7] used microarrays to distinguish numerous differentially expressed lncRNAs in skeletal muscles of OP patients. In function, lncRNAs are thought to be involved in OP by modulating osteoblast and osteoclast proliferation, apoptosis, and inflammatory responses.[8] For example, lncRNA MIR22HG was poorly expressed in MSCs from osteoporotic mice, but was considerably upregulated in MSCs after osteogenic differentiation.[9] Moreover, the overexpression of lncRNA MIR22HG overexpression promotes MSC osteogenic differentiation.[9] LINC01089, which is located in chromosome 12, has been broadly reported in cancer biology. LINC01089 has been demonstrated to play tumour-suppressive roles in lung cancer, gastric cancer, and breast cancer.[10-12] Unfortunately, its function in OP has not been addressed, and its effects on hMSC osteogenic differentiation needs to be explored.

LncRNAs may serve as molecular sponges of target microRNAs (miRNAs), thus affecting the expression of miRNA-targeted messenger RNAs (mRNAs).[8] LINC01089 was previously proposed to sponge miR-27a to upregulate SFRP1 expression, thus suppressing lung cancer tumorigenesis.[10] In view of the lack of related mechanisms of LINC01089 in OP, we exploited the downstream miRNA/mRNA signalling of LINC01089. Consequently, miR-1287-5p and its downstream functional gene heat shock protein family A (HSP70) member 4 (HSPA4), which was predicted by bioinformatics tools, were screened out in our study. A high miR-1287-5p expression has been detected in stem cells from human exfoliated deciduous teeth with high osteogenic potential.[13] Heat shock protein family proteins have been widely demonstrated to regulate osteogenic differentiation and exert diverse functional effects.[14,15] Nevertheless, the detailed functions of miR-1287-5p and HSPA4 in hMSC osteogenic differentiation need to be further validated. Furthermore, it is unclear whether the miR-1287-5p/HSPA4 axis is involved in the LINC01089 regulatory network.

The current work assayed the expression of LINC01089 in serum samples of OP patients and osteogenic differentiation-induced hMSCs. The functional effects of LINC01089 on hMSC osteogenic differentiation were explored. We first clarified if miR-1287-5p had an association with LINC01089 and HSPA4, and proposed a new mechanism regarding the function of LINC01089 on hMSC osteogenic differentiation.

Methods

Clinical specimen collection

In this work, a total of 27 blood samples from OP patients (OP group) and 27 blood samples from the non-OP patients (normal group) who suffered from external traumatic fracture were obtained in our hospital. The patients were diagnosed with OP by dual energy x-ray absorptiometry (DXA) scan and blood test. The OP patients were selected according to the following conditions: 1) all participants were only diagnosed with OP without other diseases; 2) all participants had never received any medical therapy prior to collection of their specimens; and 3) all participants provided the informed consent forms. The clinical characteristics are shown in Table I. All blood samples were cryopreserved at -80°C for subsequent quantitative reverse transcription polymerase chain reaction (RT-qPCR) analysis. This work obtained the permission of the ethics committee of Xiangyang Hospital of Integrated Traditional Chinese and Western Medicine (approval number: No. 2022006).

Cell treatment and cell culture

Procell (China) provided the hMSCs (Cat#: CP-H166) as well as the hMSC-specific growth medium (Cat#: CM-H166) in which they were cultured. The culture conditions were as follows: 37°C with 5% CO_2. To induce osteogenic differentiation, hMSCs in six-well plates were grown in hMSC osteogenic differentiation medium (Cat#: PD-014; Procell). The osteogenic differentiation medium was refreshed every three days. The hMSCs induced for the indicated time (zero, one, three, five, seven, and 14 days) were collected for study.

Cell transfection

LINC01089 overexpression vector (OE-lnc) and its matched empty vector negative control (OE-NC), short hairpin RNA (shRNA) of LINC01089 (sh-lnc) and its control (sh-NC), and siRNA of HSPA4 (sh-HSPA4) and its corresponding control (sh-NC) were all customized by GenePharma (China). The

Table I. Characteristics of all participants.

Characteristic	All subjects	
	OP patients (n = 27)	Non-OP patients (n = 27)
Mean age, yrs (SD)	58.6 (12.3)	55.2 (9.7)
Female, %	59.3	51.9
Mean BMI, kg/m^2 (SD)	23.7 (2.6)	24.1 (2.3)
Bone mineral density, T score	≤ -2.5	≥ -1
Mean calcium, mmol/l (SD)	1.7 (0.8)	2.4 (0.6)
Phosphorus, mmol/l	< 1.0	≥ 1.1

OP, osteoporosis.

miR-1287-5p mimics (miR-1287-5p-mimics, sense strand: 5′-UGCUGGAUCAGUGGUUCGAGUC-3′) used for upregulating miR-1287-5p, miRNA mimic NC (miR-NC), miR-1287-5p inhibitors (inhibitor, sense strand: 5′-GACUCGAACCACUGAUC-CAGCA-3′) used for downregulating miR-1287-5p, and miRNA inhibitor NC (inhibitor-NC) were directly bought from RiboBio (China). Lipofectamine 3000 reagents (Cat#: L3000008; Invitrogen, Thermo Fisher Scientific, USA) were used, in accordance with the protocol, for the cell transfections.

RT-qPCR

First, RNA samples were acquired using the Trizol reagent (Cat#: 15596026; Invitrogen) as the protocol suggested. Next, two commercial RT-qPCR kits specifically for lncRNA/mRNA and miRNA, namely the riboSCRIPT RT-qPCR Starter Kit (Cat#: C11030-2; RiboBio) and Bulge-Loop miRNA RT-qPCR Starter Kit (Cat#: C10211-2; RiboBio), were used for the reverse transcription and quantification. Every sample had three repeats in three duplicate wells. Glyceraldehyde 3-phosphate dehydrogenase (GAPDH) or U6 was used to normalize the data. Relative expression was obtained from the computational Ct values with the use of the $2^{-\Delta\Delta Ct}$ method. Primer information is displayed in Table II.

Subcellular location

To ascertain the nuclear and cytoplasmic distribution of LINC01089, the nuclear and cytoplasmic RNA from hMSCs was isolated with the aid of the PARIS kit (Cat#: AM1921; Invitrogen). Next, the RNA samples were investigated via RT-qPCR to determine the abundance of LINC01089 in every fraction. GAPDH was adopted as the marker for the cytoplasm while U6 was adopted for the nucleus.

Alkaline phosphatase activity assay

ALP activity was assessed using the ALP Activity Assay Kit (Cat#: E-BC-K091-S; Elabscience, China) based on colorimetric analysis. Cells were treated with homogenization medium (1 × 10^6 cells in 500 μl) and were thereafter used for sonicating. The treated cells were centrifuged to collect cellular supernatant. The following detection was conducted in line with the protocol. Finally, the optical density (OD) values (520 nm) of each sample were analyzed by a spectrophotometer (Mapada, China).

Table II. Real-time polymerase chain reaction primer synthesis list.

Gene	Sequences	
LINC01089	Forward	5′-TTTTGCCTACCCAACCCTGG-3′
	Reverse	5′-CCTGCCGTTGACAGAAGGAA-3′
miR-1287-5p	Forward	5′-ATGGAGCCCTTCAACACTTGG-3′
	Reverse	5′-AGCTGGATCAGTGGTTCGAG-3′
HSPA4	Forward	5′-AAAGATGGACCAACCACCCC-3′
	Reverse	5′-CCTCCACTGCGTTCTTAGCA-3′
RUNX2	Forward	5′-CGCCTCACAAACAACCACAG-3′
	Reverse	5′-TCACTGTGCTGAAGAGGCTG-3′
OPN	Forward	5′-CTCAGAAGCAGAATCTC-3′
	Reverse	5′-ATGGTCTCCATCGTCATCAT-3′
ALP	Forward	5′-GAGCGTCATCCCAGTGGAG-3′
	Reverse	5′-TAGCGGTTACTGTAGACACCC-3′
OCN	Forward	5′-GAGGGCAATAAGGTAGTGAA-3′
	Reverse	5′- CATAGATGCGTTTGTAGGC-3′
U6	Forward	5′-CTCGCTTCGGCAGCACA-3′
	Reverse	5′-AACGCTTCACGAATTTGCGT-3′
GAPDH	Forward	5′-AGAAAAACCTGCCAAATATGATGAC-3′
	Reverse	5′-TGGGTGTCGCTGTTGAAGTC-3′

ALP, alkaline phosphatase; GAPDH, glyceraldehyde 3-phosphate dehydrogenase; HSPA4, heat shock protein family A (HSP70) member 4; OCN, osteocalcin; OPN, osteopontin; RUNX2, runt-related transcription factor 2.

Alizarin red S staining analysis

Following the 14-day osteogenic differentiation, the hMSCs were rinsed with PBS and subsequently treated for 30 minutes with 4% paraformaldehyde for fixation. Afterward, the cells were rinsed with ddH_2O and were thereafter subjected to 30 minutes of staining with 40 mM alizarin red S (ARS) (Cat#: A5533; Sigma-Aldrich, USA). Finally, the stained calcification nodules were observed by means of light microscopy (Nikon, Japan). The amount of calcium mineral deposit was evaluated by dissolving the cell-bound ARS in 10% acetic acid followed by performing spectrophotometric quantification at a wavelength of 415 nm.

Cell Counting Kit-8 assay

To evaluate cell proliferative capacity, the hMSCs (5 × 10^3 cells/well) were inoculated on 96-well plates and maintained at 37°C. The cells were cultured for 24, 48, or 72 hours in different wells and were thereafter treated with Cell Counting Kit-8 (CCK-8) reagent (Cat#: 96992; Sigma-Aldrich) for an additional two hours. Finally, the absorbance at a wavelength of 450 nm was checked by means of an ELx800 microplate reader (BioTek, USA).

Dual-luciferase reporter study

A sequence fragment from LINC01089 or HSPA4 3′ untranslated region (3′UTR) containing the wild-type (WT) or mutant (MUT) binding site of miR-1287-5p was directly synthesized

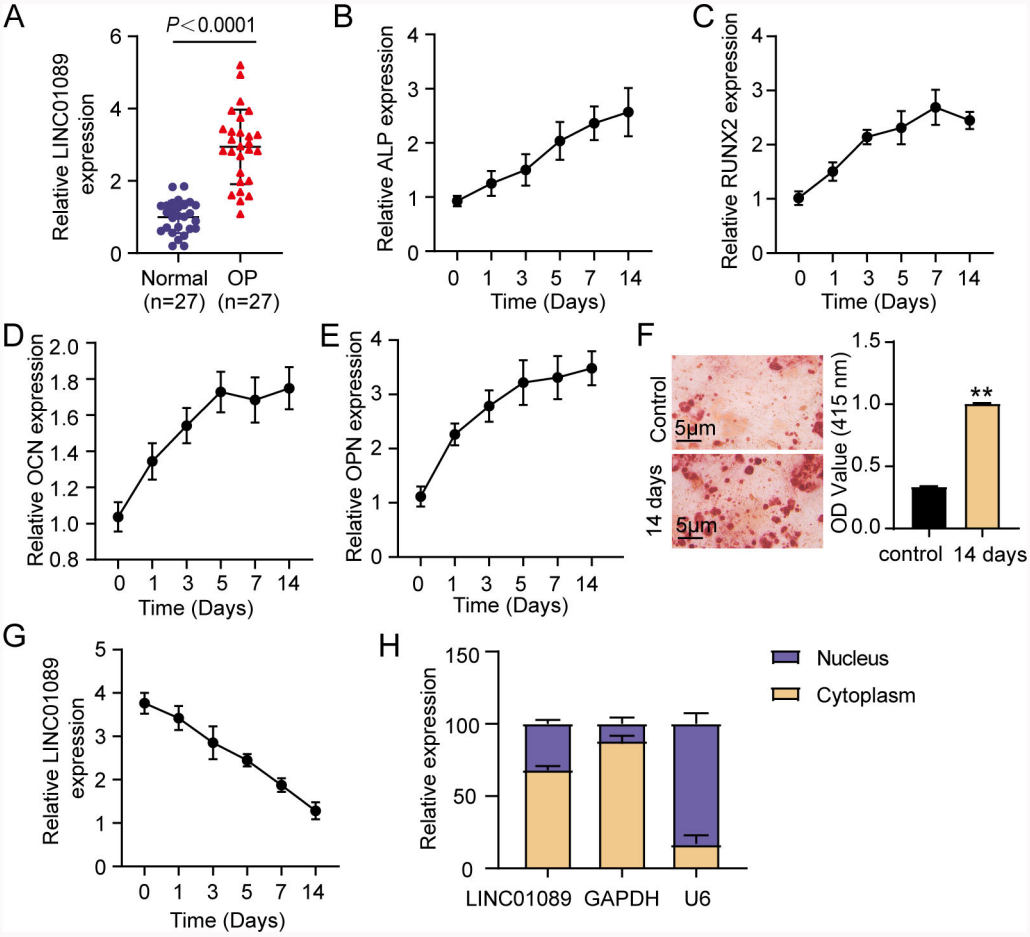

Fig. 1

LINC01089 was highly expressed in osteoporosis (OP)-derived serum samples, and its expression gradually diminished while the human mesenchymal stem cells (hMSCs) underwent osteogenic differentiation. a) LINC01089 expression in clinical samples from OP patients and normal subjects. b) to e) The levels of alkaline phosphatase (ALP), runt-related transcription factor 2 (RUNX2), osteocalcin (OCN), and osteopontin (OPN) messenger RNAs (mRNAs) in osteogenic differentiation-induced hMSCs. f) Alizarin red S (ARS) staining and quantitative analysis of calcium mineral deposition in osteogenic differentiation-induced hMSCs. **p < 0.001, one-way analysis of variance. g) LINC01089 expression in osteogenic differentiation-induced hMSCs. h) Subcellular location of LINC01089. GAPDH, glyceraldehyde 3-phosphate dehydrogenase; OD, optical density.

and subcloned into pmirGLO vector to produce LNC-WT, LNC-MUT, HSPA4-WT, and HSPA4-MUT reporter vectors. With miR-NC as the control, the miR-1287-5p mimic along with its corresponding reporter vector were transfected into hMSCs. The cells were maintained for 48 hours. Thereafter, the luciferase activity was assayed using the dual-luciferase reporter kit (Cat#: E1910; Promega, USA).

RNA immunoprecipitation experiment

A commercial RNA immunoprecipitation (RIP) Assay Kit (Cat#: 17-700; Millipore, USA) was used in this experiment. The hMSC lysates were incubated with RIP buffer and magnetic beads conjugated with anti-Ago2 or anti-immunoglobulin G (IgG) antibody. The immunoprecipitated RNAs from Ago2 and IgG (negative control) were analyzed via RT-qPCR to detect the presence of LINC01089 and miR-1287-5p.

Statistical analysis

Experimental data were obtained from three independent biological experiments. Data processing and statistical analyses were accomplished in GraphPad Prism 7 software (GraphPad, USA). The statistical differences in two groups were compared using independent-samples *t*-test, whereas the statistical differences in more than two groups were compared using one-way analysis of variance (ANOVA). A p-value < 0.05 is indicative of a statistically significant difference. Results are presented as means and SDs.

Results

LINC01089 upregulation and downregulation

Firstly, the expression pattern of LINC01089 was ascertained in OP. LINC01089 expression was considerably reinforced in OP-derived clinical samples in contrast to that in normal controls (Figure 1a). hMSCs were cultured with the osteogenic differentiation medium to induce hMSC differentiation. Several osteogenic differentiation-related markers were quantified through RT-qPCR. The ALP, RUNX2, OCN, and osteopontin (OPN) expression levels noticeably rose in osteogenic-differentiated hMSCs over time (Figures 1b to 1e). The calcium deposition increased substaconntially on the 14th day after osteogenic induction (Figure 1f). We observed that LINC01089 expression gradually decreased in hMSCs from day 0 to day 14 after the induction of osteogenic differentiation (Figure 1g). Moreover, LINC01089 was mainly located in the cytoplasm of hMSCs (Figure 1h). These data showed that

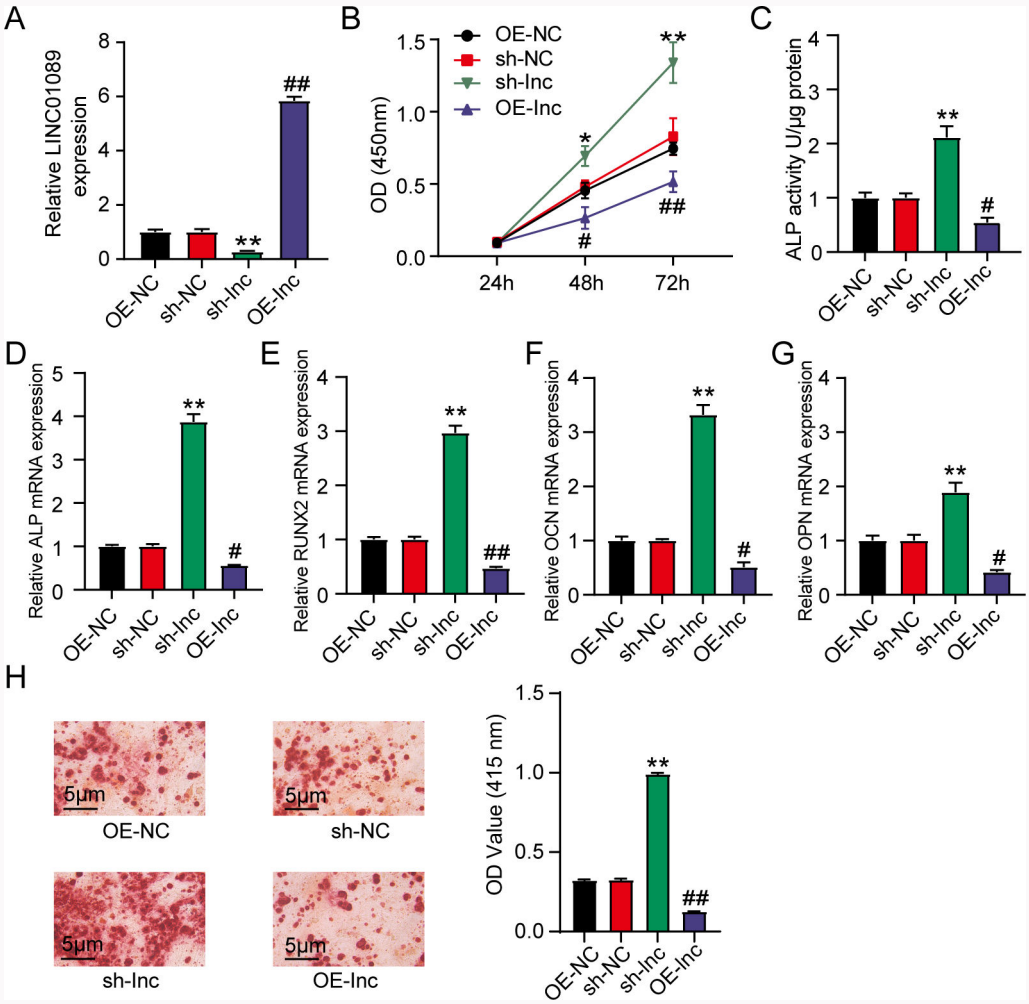

Fig. 2
LINC01089 negatively regulated human mesenchymal stem cell (hMSC) osteogenic differentiation. a) to h) Osteogenic differentiation-induced hMSCs were introduced with OE-lnc, OE-NC, sh-NC, or sh-lnc. a) LINC01089 expression in the transfected hMSCs. b) Cell proliferation in the transfected hMSCs was detected by Cell Counting Kit-8 (CCK-8) assay. c) to g) Alkaline phosphatase (ALP) activity and levels of ALP, runt-related transcription factor 2 (RUNX2), osteocalcin (OCN), and osteopontin (OPN) messenger RNAs (mRNAs) were measured to assess osteogenic differentiation. h) Alizarin red S (ARS) staining and quantitative analysis of calcium mineral deposition in the transfected hMSCs. $^{\#}p < 0.05$ and $^{\#\#}p < 0.001$ vs OE-NC; $^{*}p < 0.05$ and $^{**}p < 0.001$ vs sh-NC. All p-values were calculated using one-way analysis of variance. OD, optical density.

LINC01089 was upregulated in OP but downregulated during the osteogenic differentiation of hMSCs.

LINC01089 negatively regulates hMSC osteogenic differentiation capacity

We executed LINC01089-mediated gain- and loss-of-function experiments to investigate how LINC01089 functioned. LINC01089 abundance was markedly reduced in hMSCs after sh-lnc transfection, but considerably strengthened in hMSCs after OE-lnc transfection (Figure 2a). The cell viability curve from the CCK-8 experiment uncovered that the proliferative capacity of hMSCs after sh-lnc transfection notably improved, while the proliferative capacity of hMSCs after OE-lnc transfection considerably declined (Figure 2b). In addition, LINC01089 deficiency pronouncedly heightened ALP activity as well as ALP, RUNX2, OPN, and OCN expression levels. Meanwhile, LINC01089 upregulation resulted in a decline in ALP activity and ALP, RUNX2, OPN, and OCN expression levels (Figures 2c to 2g). Moreover, the calcium deposition noticeably increased in the sh-lnc group but weakened in the OE-lnc group (Figure 2h). These results indicate that LINC01089 repressed the osteogenesis of hMSCs.

miR-1287-5p is negatively modulated by LINC01089

OP-derived clinical samples manifested a notable decline in miR-1287-5p expression in contrast to normal controls (Figure 3a). LINC01089 expression in OP-derived clinical samples showed a negative association with that of miR-1287-5p (Figure 3b). From days 0 to 14 after the induction of osteogenic differentiation, a gradual increase in miR-1287-5p expression was detected in hMSCs (Figure 3c). Figure 3d depicts the starBase-predicted binding site between LINC01089 and miR-1287-5p. The binding site was verified by the dual-luciferase reporter data, which indicated that luciferase activity was greatly declined in hMSCs after the co-transfection of miR-1287-5p and LNC-WT but not LNC-MUT (Figure 3e). Furthermore, we observed that LINC01089 and miR-1287-5p were richly expressed in Ago2-captured RNA complexes relative to those of IgG (Figure 3f). Subsequently, miR-1287-5p inhibitor was transfected into sh-lnc-transfected

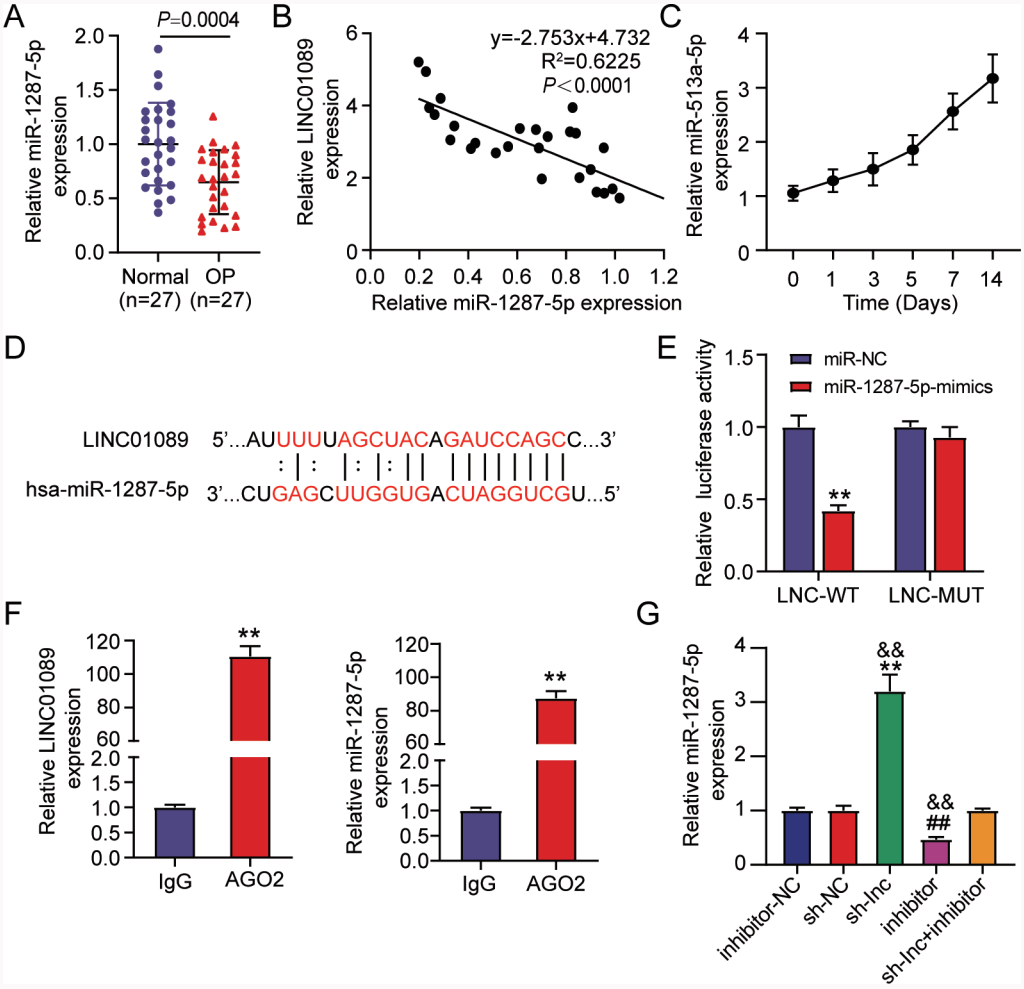

Fig. 3

miR-1287-5p was targeted by LINC01089 and negatively modulated by LINC01089. a) miR-1287-5p expression in clinical samples of osteoporosis (OP) patients and normal subjects. b) The correlation of LINC01089 expression with that of miR-1287-5p in OP-derived clinical samples. c) miR-1287-5p expression in osteogenic differentiation-induced human mesenchymal stem cells (hMSCs). d) The starBase predicted miR-1287-5p–LINC01089 binding site. e) and f) The potential binding of LINC01089 with miR-1287-5p was ensured through the dual-luciferase reporter study (**p < 0.001 vs miR-NC) and RNA immunoprecipitation (RIP) assay (**p < 0.001 vs IgG). g) miR-1287-5p expression in hMSCs that contain sh-NC, sh-lnc, inhibitor-NC, inhibitor, or sh-lnc+ inhibitor. ##p < 0.001 vs inhibitor-NC; **p < 0.001 vs sh-NC; &&p < 0.001 vs sh-lnc + inhibitor. All p-values were calculated using one-way analysis of variance. IgG, immunoglobulin G; MUT, mutant; WT, wild-type.

hMSCs for rescue experiments. Cells with sh-lnc + inhibitor transfection exhibited a substantial impairment in miR-1287-5p expression relative to those with sh-lnc transfection instead (Figure 3g). This suggests that LINC01089 knockdown enriched miR-1287-5p.

miR-1287-5p depletion

In rescue experiments, miR-1287-5p inhibitor repressed the hMSC proliferative capacity considerably, while the LINC01089-absence-strengthened cell proliferative capacity was notably weakened by further miR-1287-5p depletion (Figure 4a). ALP activity was markedly reduced in hMSCs with miR-1287-5p depletion, while the LINC01089 absence-induced increase in ALP activity was substantially repressed by the miR-1287-5p depletion (Figure 4b). As expected, the expression of ALP, RUNX2, OCN, and OPN was remarkably depleted by the presence of the inhibitor of miR-1287-5p in hMSCs (Figures 4c to 4f). Moreover, their expression levels were notably impaired by the sh-lnc + inhibitor transfection relative to the sh-lnc transfection in hMSCs (Figures 4c to 4f). Accordingly, the calcium deposition was markedly repressed in hMSCs upon the depletion of miR-1287-5p, and the LINC01089 absence-strengthened ARS staining level was considerably reversed by the miR-1287-5p depletion (Figure 4g). The data revealed that LINC01089 absence promoted hMSC osteogenic differentiation via miR-942-5p targeting.

HSPA4 is a downstream molecule of the LINC01089/miR-1287-5p pathway

HSPA4 expression was upregulated in OP-derived clinical samples relative to normal controls (Figure 5a). Besides, the HSPA4 expression in OP-derived clinical samples was inversely associated with the expression of miR-1287-5p but was positively associated with that of LINC01089 (Figures 5b and 5c). Figure 5d shows the TargetScan-predicted putative binding site of HSPA4 3'UTR and miR-1287-5p. HSPA4 expression gradually declined in hMSCs from day 0 to day 14 after the induction of osteogenic differentiation (Figure 5e). The decreased luciferase activity in hMSCs transfected with a combination of miR-1287-5p, and HSPA4-WT further

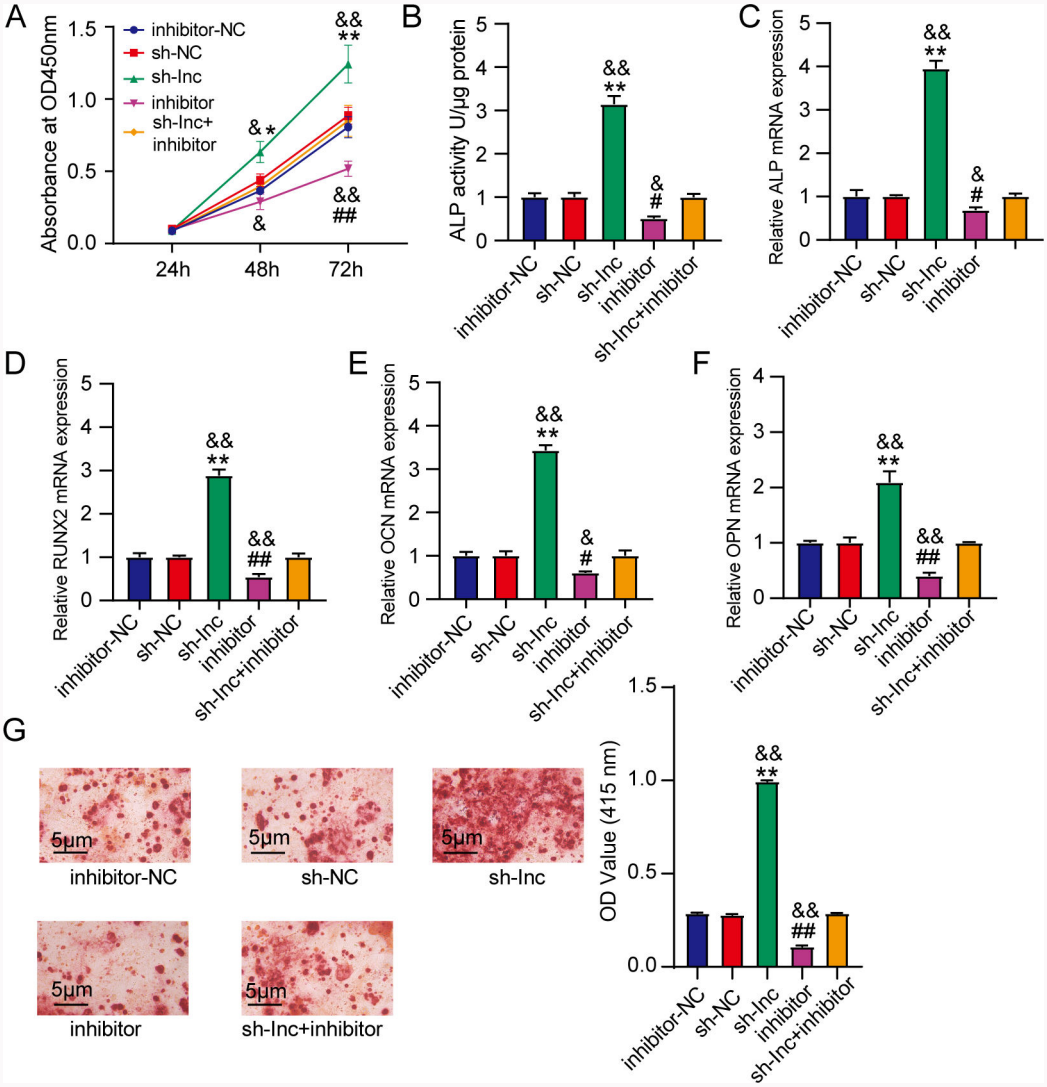

Fig. 4

miR-1287-5p inhibition reversed the effects of LINC01089 absence. a) to g) Osteogenic differentiation-induced human mesenchymal stem cells (hMSCs) were introduced with sh-NC, sh-lnc, inhibitor-NC, inhibitor, or sh-lnc + inhibitor. a) Cell proliferation was evaluated by Cell Counting Kit-8 (CCK-8) assay. b) to f) Alkaline phosphatase (ALP) activity and the messenger RNA (mRNA) levels of ALP, runt-related transcription factor 2 (RUNX2), osteocalcin (OCN), and osteopontin (OPN) were measured to assess osteogenic differentiation. g) Alizarin red S (ARS) staining and quantitative analysis of calcium mineral deposition in the transfected hMSCs. $^{\#}p < 0.05$ and $^{\#\#}p < 0.001$ vs inhibitor-NC; $^{*}p < 0.05$ and $^{**}p < 0.001$ vs sh-NC; $^{\&}p < 0.05$ and $^{\&\&}p < 0.001$ vs sh-lnc + inhibitor. All p-values were calculated using one-way analysis of variance. OD, optical density.

substantiated the miR-1287-5p–HSPA4 3'UTR binding site (Figure 5f). HSPA4 mRNA level was markedly improved in hMSCs after the miR-1287-5p inhibitor transfection, but was greatly weakened by sh-HSPA4 transfection (Figure 5g). Furthermore, the miR-1287-5p inhibitor partly restored the sh-HSPA4-reduced HSPA4 expression (Figure 5g), implying that miR-1287-5p negatively modulated HSPA4 expression.

The promotive effects of HSPA4 knockdown on hMSC osteogenic differentiation

We investigated the functional effects of knocking down HSPA4, and then performed rescue experiments. As exhibited in Figure 6a, HSPA4 knockdown remarkably enhanced cell proliferative capacity, while further miR-1287-5p depletion partly impaired the cell proliferation which was induced by the HSPA4 knockdown. The HSPA4 knockdown-strengthened ALP activity was considerably repressed by additional miR-1287-5p inhibition (Figure 6b). The levels of ALP, RUNX2, OPN, and OCN mRNA were notably reinforced by sh-HSPA4 in hMSCs. Meanwhile, the miR-1287-5p inhibitor abolished, at least in part, the influence of sh-HSPA4 on ALP, RUNX2, OCN, and OPN (Figures 6c to 6f). The calcium deposition remarkably improved in hMSCs with sh-HSPA4, but was partly repressed in hMSCs with sh-HSPA4+ inhibitor (Figure 6g). These observations indicate that HSPA4 knockdown enhances hMSC osteogenic differentiation capacity, and miR-1287-5p inhibition can abolish, at least in part, the influences of HSPA4 knockdown.

Discussion

The present study monitored the upregulation of LINC01089 in OP serum samples and the gradual decrease of LINC01089 expression in hMSCs during osteogenic differentiation. The aberrant expression of LINC01089 hinted that LINC01089 was involved in OP pathological progress. Gain- and loss-of-function assays identified that LINC01089 knockdown induced

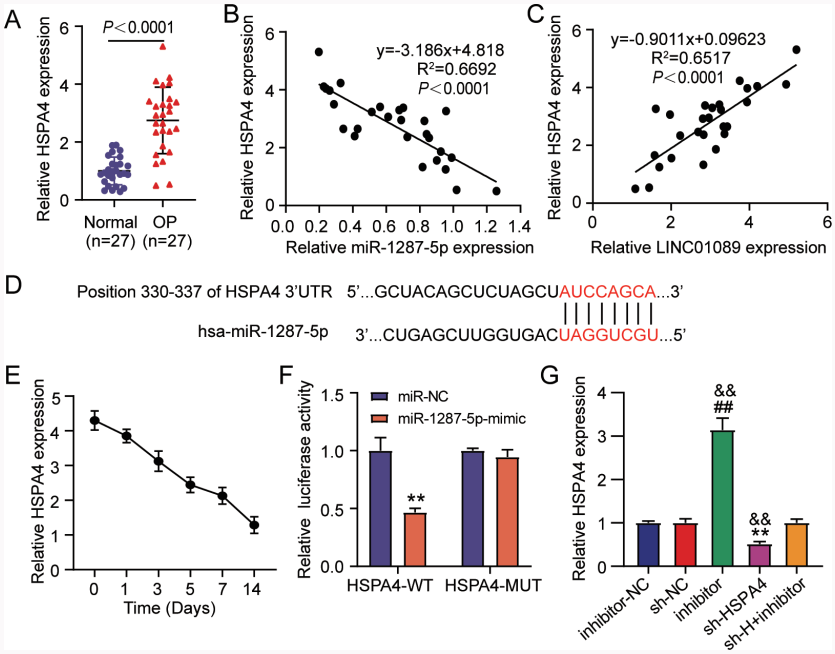

Fig. 5

Heat shock protein family A (HSP70) member 4 (HSPA4) was LINC01089/miR-1287-5p pathway's downstream gene. a) HSPA4 expression in clinical samples of osteoporosis (OP) patients and normal subjects. b) and c) The correlation of HSPA4 expression with that of LINC01089 and miR-1287-5p in OP-derived clinical samples. d) The TargetScan-predicted binding site between miR-1287-5p and HSPA4 3'UTR. e) HSPA4 expression in osteogenic differentiation-induced human mesenchymal stem cells (hMSCs). f) The binding between miR-1287-5p and HSPA4 was ensured by dual-luciferase reporter study. **p < 0.001 vs miR-NC. g) The expression of HSPA4 messenger RNA (mRNA) in hMSCs transfected with inhibitor, inhibitor-NC, sh-HSPA4, sh-NC, or sh-HSPA4+ inhibitor. **p < 0.001 vs sh-NC; ##p < 0.01 vs inhibitor-NC; &&p < 0.001 vs sh-H + inhibitor (sh-H: sh-HSPA4). All p-values were calculated using one-way analysis of variance.

hMSC osteogenic differentiation, which was partly attributed to the regulation of LINC01089 on miR-1287-5p/HSPA4 signalling. Our findings have been the first to unveil the function of LINC01089 in hMSC osteogenic differentiation (Figure 7), which provides a basis for the involvement of LINC01089 in OP development.

Accumulating studies have confirmed that lncRNAs serve as crucial regulators of osteogenic differentiation during the pathological progression of OP.[6–9] For instance, lncRNA MEG3 expression was found to be notably elevated in hMSCs isolated from patients suffering from OP, but its expression declined while the hMSCs underwent osteogenic differentiation.[16] MEG3 upregulation diminished the expression of RUNX2, OCN, and OPN, and impaired ALP activity to repress hMSC osteogenic differentiation.[16] However, H19 has been poorly expressed in patients with OP, and the forced expression of H19 largely stimulated hMSC osteogenic differentiation by governing its downstream signalling.[17] A study by Li[18] found that LncRNA PCBP1-AS1 was overexpressed in OP to inhibit hMSC osteogenic differentiation. As for LINC01089, it has been previously declared to be a tumour inhibitor in various cancers.[19-22] LINC01089 was weakly expressed in colorectal cancer, and its upregulation restrained cancer cell growth and invasion.[19] The poor expression of LINC01089 was also identified in gastric cancer, and further depletion of LINC01089 aggravated gastric cancer cell growth and metastasis.[20] Interestingly, we observed that LINC01089 expression was noticeably reinforced in serum samples acquired from patients suffering from OP. Moreover, its expression was progressively diminished in hMSCs during osteogenic differentiation. Regarding its function, we uncovered that LINC01089 knockdown promotes hMSC osteogenic differentiation. This was evidenced by the increase in ALP activity, ARS staining, and expression of RUNX2, OCN, and OPN. LINC01089 overexpression showed the opposite effects, indicating that LINC01089 negatively regulates hMSC osteogenic differentiation and may promote the development of OP.

Regarding the functional mechanism of LINC01089 in cancer biology, LINC01089 has been verified to act as competing endogenous RNA to drive the miRNA/mRNA networks.[10,22,23] Numerous miRNAs that had been predicted to be potential targets of LINC01089 have not been validated. The binding of LINC01089 with miR-1287-5p was verified in our study via multiple tests. It is well studied that miR-1287-5p exerts tumour-suppressive effects in diverse cancers.[24-26] For example, miR-1287-5p has the potential to repress breast cancer cell aggressive phenotypes and breast tumour formation and growth in animal models.[24] miR-1287-5p has also been reported to have an elevated expression in stem cells of human exfoliated deciduous teeth with high osteogenic potential.[13] In addition, miR-1287-5p negatively regulates CD105 expression, and a low CD105 expression is associated with increased expression of RUNX2 and ALP.[13] Our data found that miR-1287-5p depletion inhibits hMSC proliferation; reduces ALP, RUNX2, OPN, and OCN expression; and impairs ARS staining level, indicating that miR-1287-5p depletion may repress hMSC osteogenic differentiation. Moreover, the rescue experiments demonstrated that miR-1287-5p depletion largely overturns the effects of LINC01089 absence, supporting that LINC01089 targets miR-1287-5p to regulate hMSC osteogenic differentiation.

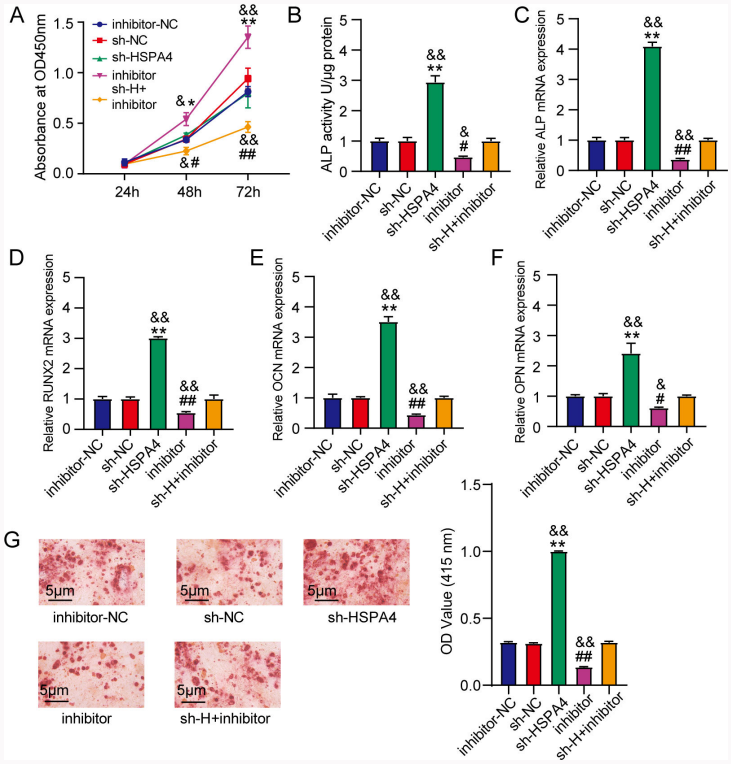

Fig. 6

The inhibition of miR-1287-5p abolished the effect of heat shock protein family A (HSP70) member 4 (HSPA4) knockdown. a) to g) Osteogenic differentiation-induced human mesenchymal stem cells (hMSCs) were introduced with inhibitor, inhibitor-NC, sh-HSPA4, sh-NC, or sh-HSPA4+ inhibitor. a) The proliferation of the transfected cells was evaluated via the Cell Counting Kit-8 (CCK-8) assay. b) to f) Among the transfected cells, alkaline phosphatase (ALP) activity and levels of ALP, runt-related transcription factor 2 (RUNX2), osteocalcin (OCN), and osteopontin (OPN) messenger RNAs (mRNAs) were measured to assess osteogenic differentiation. g) Alizarin red S (ARS) staining and quantitative analysis of calcium mineral deposition in the transfected hMSCs. $^{\#}p < 0.05$ and $^{\#\#}p < 0.001$ vs inhibitor-NC; $^{*}p < 0.05$ and $^{**}p < 0.001$ vs sh-NC; $^{\&}p < 0.05$ and $^{\&\&}p < 0.001$ vs sh-H+ inhibitor (sh-H: sh-HSPA4). OD, optical density. All p-values were calculated using one-way analysis of variance.

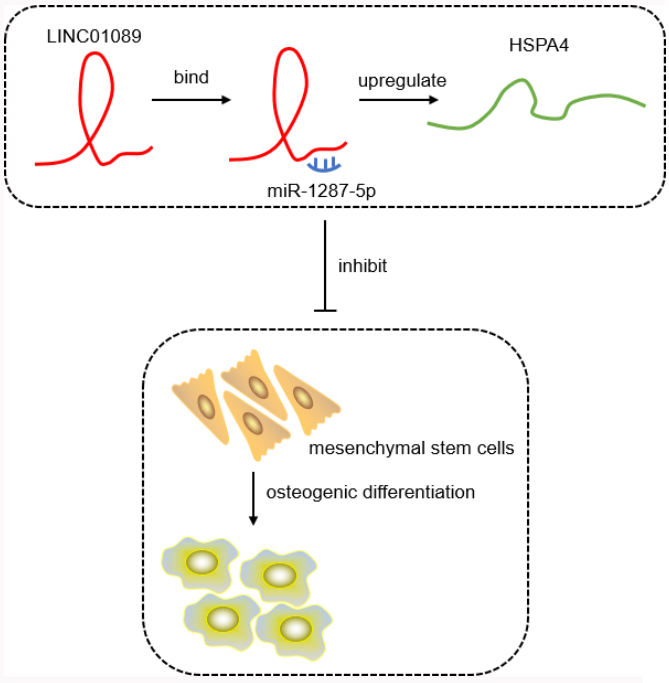

Fig. 7

The role of LINC01089 in human mesenchymal stem cell osteogenic differentiation. HSPA4, heat shock protein family A (HSP70) member 4.

To further understand the regulatory network of LINC01089, the downstream functional genes targeted by miR-1287-5p were identified. We observed that HSPA4 expression is elevated in OP-derived serum samples, but it also diminishes gradually in hMSCs during osteogenic differentiation, thereby garnering our attention. We subsequently verified if miR-1287-5p binds with HSPA4 3'UTR and discovered that miR-1287-5p negatively regulates HSPA4 expression. The functional role of HSPA4 on hMSC osteogenic differentiation has not yet been explored. Reviewing the existing studies, we discovered that other members of heat shock protein family play crucial roles in osteogenic differentiation, such as HSPB7 and HSP70.[14,27] HSPB7 is poorly expressed in human adipose-derived stem cells during osteogenic differentiation, while HSP70 expression is elevated in hMSCs during osteogenic differentiation,[14,27] suggesting that heat shock protein family members exert diverse functional effects. This work is the first to show the potential effects of HSPA4 on hMSC osteogenic differentiation, demonstrating that HSPA4 downregulation restrains hMSC osteogenic differentiation by depleting ALP activity, ARS staining level, and the expression of ALP, RUNX2, OCN, and OPN. Moreover, the introduction of miR-1287-5p inhibitor attenuated, at least in part, the influence of HSPA4 downregulation, indicating that miR-1287-5p influences the function of HSPA4.

In conclusion, we collectively discovered for the first time that LINC01089 expression is notably reduced

in hMSCs during osteogenic differentiation. LINC01089 overexpression represses hMSC osteogenic differentiation, and LINC01089 absence promotes hMSC osteogenic differentiation. LINC01089 exerts these effects by targeting the miR-1287-5p/HSPA4 signalling pathway. Our research is a preliminary study that introduces the role of LINC01089 on hMSC osteogenic differentiation in vitro, implying that LINC01089 may be a novel target for OP intervention, which strongly needs to be validated in future animal models.

References

1. **Jiang Y**, **Zhang P**, **Zhang X**, **Lv L**, **Zhou Y**. Advances in mesenchymal stem cell transplantation for the treatment of osteoporosis. *Cell Prolif*. 2021;54(1):e12956.
2. **Xu F**, **Li W**, **Yang X**, **Na L**, **Chen L**, **Liu G**. The roles of epigenetics regulation in bone metabolism and osteoporosis. *Front Cell Dev Biol*. 2020;8:619301.
3. **Kenkre JS**, **Bassett J**. The bone remodelling cycle. *Ann Clin Biochem*. 2018;55(3):308–327.
4. **Siris ES**, **Adler R**, **Bilezikian J**, **et al**. The clinical diagnosis of osteoporosis: a position statement from the National Bone Health Alliance Working Group. *Osteoporos Int*. 2014;25(5):1439–1443.
5. **Arthur A**, **Gronthos S**. Clinical application of bone marrow mesenchymal stem/stromal cells to repair skeletal tissue. *Int J Mol Sci*. 2020;21(24):9759.
6. **Li Y**, **Li J**, **Chen L**, **Xu L**. The roles of long non-coding RNA in osteoporosis. *Curr Stem Cell Res Ther*. 2020;15(7):639–645.
7. **Liu S**, **Huang H**, **Chai S**, **Wei H**, **Huang J**, **Wan L**. Expression profile analysis of long non-coding RNA in skeletal muscle of osteoporosis by microarray and bioinformatics. *J Biol Eng*. 2019;13:50.
8. **Ko N-Y**, **Chen L-R**, **Chen K-H**. The role of micro RNA and long-non-coding RNA in osteoporosis. *Int J Mol Sci*. 2020;21(14):4886.
9. **Jin C**, **Jia L**, **Tang Z**, **Zheng Y**. Long non-coding RNA MIR22HG promotes osteogenic differentiation of bone marrow mesenchymal stem cells via PTEN/ AKT pathway. *Cell Death Dis*. 2020;11(7):601.
10. **Li X**, **Lv F**, **Li F**, **et al**. LINC01089 inhibits tumorigenesis and epithelial-mesenchymal transition of non-small cell lung cancer *via* the miR-27a/SFRP1/Wnt/β-catenin axis. *Front Oncol*. 2020;10:532581.
11. **Yang F**, **Chen X**, **Li X**, **et al**. Long intergenic non-protein coding RNA 1089 suppresses cell proliferation and metastasis in gastric cancer by regulating miRNA-27a-3p/epithelial-mesenchymal transition (EMT) axis. *Cancer Manag Res*. 2020;12:5587–5596.
12. **Yuan H**, **Qin Y**, **Zeng B**, **et al**. Long noncoding RNA LINC01089 predicts clinical prognosis and inhibits cell proliferation and invasion through the Wnt/β-catenin signaling pathway in breast cancer. *Onco Targets Ther*. 2019;12:4883–4895.
13. **Ishiy FAA**, **Fanganiello RD**, **Kobayashi GS**, **Kague E**, **Kuriki PS**, **Passos-Bueno MR**. CD105 is regulated by hsa-miR-1287 and its expression is inversely correlated with osteopotential in SHED. *Bone*. 2018;106:112–120.
14. **Jin C**, **Shuai T**, **Tang Z**. HSPB7 regulates osteogenic differentiation of human adipose derived stem cells via ERK signaling pathway. *Stem Cell Res Ther*. 2020;11(1):450.
15. **Flanagan M**, **Li C**, **Dietrich MA**, **Richard M**, **Yao S**. Downregulation of heat shock protein B8 decreases osteogenic differentiation potential of dental pulp stem cells during in vitro proliferation. *Cell Prolif*. 2018;51(2):e12420.
16. **Wang Q**, **Li Y**, **Zhang Y**, **et al**. LncRNA MEG3 inhibited osteogenic differentiation of bone marrow mesenchymal stem cells from postmenopausal osteoporosis by targeting miR-133a-3p. *Biomed Pharmacother*. 2017;89:1178–1186.
17. **Li T**, **Jiang H**, **Li Y**, **Zhao X**, **Ding H**. Estrogen promotes lncRNA H19 expression to regulate osteogenic differentiation of BMSCs and reduce osteoporosis via miR-532-3p/SIRT1 axis. *Mol Cell Endocrinol*. 2021;527:111171.
18. **Li Z**. LncRNA PCBP1-AS1 induces osteoporosis by sponging miR-126-5p/PAK2 axis. *Bone Joint Res*. 2023;12(6):375–386.
19. **Li M**, **Guo X**. LINC01089 blocks the proliferation and metastasis of colorectal cancer cells via regulating miR-27b-3p/HOXA10 axis. *Onco Targets Ther*. 2020;13:8251–8260.
20. **Guo X**, **Li M**. LINC01089 is a tumor-suppressive lncRNA in gastric cancer and it regulates miR-27a-3p/TET1 axis. *Cancer Cell Int*. 2020;20:507.
21. **Li S**, **Han Y**, **Liang X**, **Zhao M**. LINC01089 inhibits the progression of cervical cancer via inhibiting miR-27a-3p and increasing BTG2. *J Gene Med*. 2021;23(1):e3280.
22. **Zhang H**, **Zhang H**, **Li X**, **Huang S**, **Guo Q**, **Geng D**. LINC01089 functions as a ceRNA for miR-152-3p to inhibit non-small lung cancer progression through regulating PTEN. *Cancer Cell Int*. 2021;21(1):143.
23. **Zhang D**, **Cai X**, **Cai S**, **Chen W**, **Hu C**. Long intergenic non-protein coding RNA 01089 weakens tumor proliferation, migration, and invasion by sponging miR-3187-3p in non-small cell lung cancer. *Cancer Manag Res*. 2020;12:12151–12162.
24. **Schwarzenbacher D**, **Klec C**, **Pasculli B**, **et al**. MiR-1287-5p inhibits triple negative breast cancer growth by interaction with phosphoinositide 3-kinase CB, thereby sensitizing cells for PI3Kinase inhibitors. *Breast Cancer Res*. 2019;21(1):20.
25. **Hao W**, **Zhu Y**, **Guo Y**, **Wang H**. miR-1287-5p upregulation inhibits the EMT and pro-inflammatory cytokines in LPS-induced human nasal epithelial cells (HNECs). *Transpl Immunol*. 2021;68:101429.
26. **Ji F**, **Du R**, **Chen T**, **et al**. Circular RNA circSLC26A4 accelerates cervical cancer progression via miR-1287-5p/HOXA7 axis. *Mol Ther Nucleic Acids*. 2020;19:413–420.
27. **Chen E**, **Xue D**, **Zhang W**, **Lin F**, **Pan Z**. Extracellular heat shock protein 70 promotes osteogenesis of human mesenchymal stem cells through activation of the ERK signaling pathway. *FEBS Lett*. 2015;589(24 Pt B):4088–4096.

Author information

H. Zou, MSc, Associate Chief Physician
F. Hu, MSc, Resident Doctor
X. Wu, BSc, Attending Doctor
B. Xu, MSc, Attending Doctor
G. Shang, BSc, Attending Doctor
D. An, BSc, Resident Doctor
D. Qin, BSc, Attending Doctor
X. Zhang, MSc, Resident Doctor
Department of Orthopedics, Xiangyang Hospital of Integrated Traditional Chinese and Western Medicine, Xiangyang, China.

A. Yang, MD, Associate Chief Physician, Department of Orthopedics, Hubei Provincial Hospital of Traditional Chinese Medicine, Wuhan, China; Department of Orthopedics, Afliated Hospital of Hubei University of Chinese Medicine, Wuhan, China.

Author contributions

H. Zou: Conceptualization, Data curation, Resources, Writing – original draft, Writing – review & editing.
F. Hu: Conceptualization, Resources, Writing – original draft, Writing – review & editing.
X. Wu: Writing – review & editing, Formal analysis, Software.
B. Xu: Supervision, Validation.
G. Shang: Investigation, Visualization.
D. An: Methodology, Project administration.
D. Qin: Investigation, Project administration.
X. Zhang: Investigation, Supervision.
A. Yang: Formal analysis, Funding acquisition.

H. Zou and F. Hu contributed equally to this work.

Funding statement

The authors disclose receipt of the following financial or material support for the research, authorship, and/or publication of this

article: this work is funded by the research project of traditional Chinese medicine from Hubei Administration of Traditional Chinese Medicine (grant number: ZY2023M043), as reported by A. Yang.

ICMJE COI statement

A. Yang reports funding from the research project of traditional Chinese medicine from Hubei Administration of Traditional Chinese Medicine (grant number: ZY2023M043), related to this study.

Data sharing

All data generated or analyzed during this study are included in the published article and/or in the supplementary material.

Acknowledgements

The study's participants granted their approval for publication, and a written informed consent form was filled out by each patient.

Ethical review statement

The medical ethics committee of Xiangyang Hospital of Integrated Traditional Chinese and Western Medicine approved this study (Xiangyang, China) (approval number: No.2022006). The clinical tissue samples were handled as instructed in ethical standards outlined in the Declaration of Helsinki. Each patient signed a document requesting their informed permission.

Open access funding

The authors report that the open access funding for their manuscript was self-funded.